Quantification of Myocardial Blood Flow With Ultrasound-Induced Destruction of Microbubbles Administered as a Constant Venous Infusion

Kevin Wei, Ananda R. Jayaweera, Soroosh Firoozan, Andre Linka, Danny M. Skyba and Sanjiv Kaul

Circulation 1998;97;473-483
Circulation is published by the American Heart Association. 7272 Greenville Avenue, Dallas, TX 72514
 Print ISSN: 0009-7322. Online ISSN: 1524-4539

Quantification of Myocardial Blood Flow With Ultrasound-Induced Destruction of Microbubbles Administered as a Constant Venous Infusion

Kevin Wei, MD; Ananda R. Jayaweera, PhD; Soroosh Firoozan, MD; Andre Linka, MD; Danny M. Skyba, PhD; Sanjiv Kaul, MD

Background—Ultrasound can cause microbubble destruction. If microbubbles are administered as a continuous infusion, then their destruction within the myocardium and measurement of their myocardial reappearance rate at steady state will provide a measure of mean myocardial microbubble velocity. Conversely, measurement of their myocardial concentration at steady state will provide an assessment of microvascular cross-sectional area. Myocardial blood flow (MBF) can then be calculated from the product of the two.

Methods and Results—Ex vivo and in vitro experiments were performed in which either flow was held constant and pulsing interval (interval between microbubble destruction and replenishment) was altered, or vice versa. In vivo experiments were performed in 21 dogs. In group 1 dogs (n=7), MBF was mechanically altered in a model in which coronary blood volume was constant. In group 2 dogs (n=5), MBF was altered by direct coronary infusions of vasodilators. In group 3 dogs (n=9), non–flow-limiting coronary stenoses were created, and MBF was measured before and after the venous administration of a coronary vasodilator. In all experiments, microbubbles were delivered as a constant infusion, and myocardial contrast echocardiography was performed using different pulsing intervals. The myocardial video intensity versus pulsing interval plots were fitted to an exponential function: $y=A(1-e^{-\beta t})$, where A is the plateau video intensity reflecting the microvascular cross-sectional area, and β reflects the rate of rise of video intensity and, hence, microbubble velocity. Excellent correlations were found between flow and β, as well as flow and the product of A and β.

Conclusions—MBF can be quantified with myocardial contrast echocardiography during a venous infusion of microbubbles. This novel approach has potential for measuring tissue perfusion in any organ accessible to ultrasound. **(*Circulation*. 1998;97:473-483.)**

Key Words: echocardiography ■ contrast media ■ blood flow ■ microcirculation

We have previously shown that the relation between MBF and total CBV can be quantified with MCE.[1,2] CBV includes the blood volume from epicardial conduit arteries, arterioles, capillaries, venules, and veins. When sonicated albumin microbubbles were injected directly into a coronary artery,[1,2] changes in the mean myocardial transit rates were found to reflect changes in the MBF/CBV relation, which is consistent with classic indicator dilution principles. This approach is limited, however, because alterations in the mean microbubble transit rate reflect relative rather than absolute changes in MBF or CBV. It is not possible to quantify one without knowing the other. The need to use intracoronary injections also limits the clinical applications of this technique.

A number of recent advances have made myocardial opacification possible through a venous injection of microbubbles. Air-filled microbubbles rapidly decrease in size in the circulation because the highly diffusible oxygen and nitrogen leak out of the bubbles and, being soluble, dissolve in blood. Because the backscatter of a bubble is related to the sixth power of its radius,[3] even a small decrease in size causes a large decrease in backscatter. Myocardial opacification is therefore not seen when air-filled bubbles are injected intravenously. This limitation has been overcome with the development of "second-generation" bubbles that contain high-molecular-weight gases that are nondiffusible and less soluble. These bubbles do not change their size appreciably after entering the systemic circulation and thus retain their backscattering properties. Their venous administration has been shown to result in successful myocardial opacification.[4–8]

We have recently shown that exposure of microbubbles to ultrasound results in their destruction.[9] This effect could be related to the induction of nonlinear oscillations in the microbubbles or represent a nonspecific effect related to the acoustic power. Regardless of the exact mechanism of ultra-

Received July 7, 1997; revision received September 30, 1997; accepted September 30, 1997.

From the Cardiovascular Division, University of Virginia School of Medicine (Charlottesville).

Presented in part at the Young Investigator Award Competition at the 46th Annual Scientific Sessions of the American College of Cardiology, March 1997, Anaheim, Calif, and in part at the 70th Annual Scientific Sessions of the American Heart Association, November 1997, Orlando, Fla.

Correspondence to Sanjiv Kaul, MD, Cardiovascular Division, Medical Center, Box 158, University of Virginia, Charlottesville, VA 22908.
E-mail sk@virginia.edu

Selected Abbreviations and Acronyms

CBV = coronary blood volume
CSA = cross-sectional area
MBF = myocardial blood flow
MBV = myocardial blood volume
MCE = myocardial contrast echocardiography
LAD = left anterior descending coronary artery
LCx = left circumflex coronary artery
LV = left ventricular, ventricle
PI = pulsing interval
VI = video intensity

sound-induced microbubble destruction, the acoustic emissions from oscillating or imploding microbubbles contain harmonics of the frequency to which the bubbles were initially exposed.[10,11] Because harmonic signals emanate mostly from bubbles rather than tissue, selective reception of these signals results in an increased signal-to-noise ratio.[4,5,9,12]

For this study, we hypothesized that ultrasound-induced destruction of intravenously delivered bubbles can be used to quantify myocardial perfusion. If microbubbles are administered as a continuous infusion, then their destruction within the myocardium and measurement of their reappearance rate will provide a measure of mean myocardial microbubble velocity. Furthermore, the microbubble concentration in the myocardium during steady state will reflect the sum of the myocardial microvascular CSA. Knowing both the mean myocardial microbubble velocity and the myocardial microvascular CSA can then provide a measure of MBF. We tested these hypotheses in ex vivo, in vitro, and in vivo experiments.

Methods

Model Development

Assume, first, that microbubbles are administered intravenously as a continuous infusion at a constant rate and concentration. After steady state is achieved, assume that all microbubbles within an ultrasound field are destroyed by a single ultrasound pulse (Fig 1) and that the elevation (thickness) of the ultrasound beam E is uniform. If new microbubbles enter this field with a flat profile at a velocity v, then the distance (d) they will travel within the beam elevation (Fig 1B through 1E) will be given by the following equation:

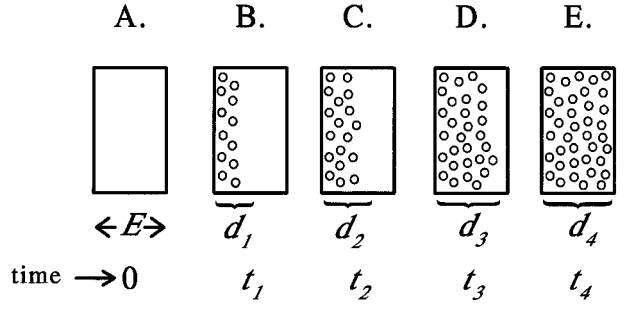

Figure 1. The elevation (thickness) of the ultrasound beam is represented as E (A). If all the microbubbles in the elevation are destroyed by a single pulse of ultrasound at t_0, then replenishment of the beam elevation (d_1 through d_4, B through E), will depend on the velocity of microbubbles and the ultrasound PI t. See text for details.

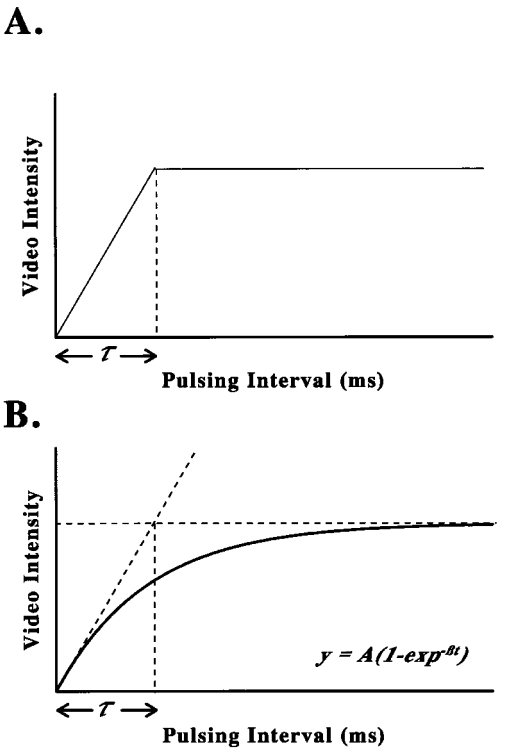

Figure 2. The PI (x axis) versus VI (y axis) relation as (A) predicted by the model and (B) observed experimentally. The function is used to derive parameters A and β. See text for details.

$$d = vt \quad (1)$$

where t is the PI of ultrasound.

Because VI is proportional to the effective microbubble concentration within the beam thickness at any PI (when the relation between the two is linear[13]), it will be proportional to d/E. Substituting for d, from equation 1, VI is proportional to vt/E. At a constant v, VI increases with t until a specific PI, T, is reached (Fig 2A), at which the microbubbles have just sufficient time to fill the entire beam thickness (Fig 1E). Then,

$$E = vT \quad (2)$$

As shown in Fig 2A, when the PI exceeds T, VI will remain constant. This plateau phase will reflect the effective microbubble concentration within the myocardial microcirculation. At any given concentration of intravenously infused microbubbles, the VI at the plateau phase will be proportional to the sum of CSA of microvessels (a) within the beam thickness.

The model predicts a sharp demarcation between the upslope and plateau phases of the PI-VI relation (Fig 2A). In reality, however, neither the beam elevation nor the degree of microbubble destruction are expected to be entirely uniform. The profile of the microbubbles also is not expected to be entirely flat. The actual relation between VI and PI is therefore more likely to be curvilinear as shown in Fig 2B and can be described by the following exponential function:

$$y = A(1 - e^{-\beta t}) \quad (3)$$

where y is VI at a PI t, A is the plateau VI, and β is the rate constant that determines the rate of rise of VI.

Because the slope of the tangent to the curves is given by $dv/dt = A\beta E^{-\beta t}$, the slope at the origin ($t=0$) is $A\beta$. As shown in Fig 2A, this slope is also equal to A/T. Therefore,

$$T = 1/\beta \quad (4)$$

Eliminating T between equations 2 and 4 results in:

(5) $$v = E\beta$$

Thus, for a given beam elevation (thickness at a given distance from the transducer), the mean velocity of microbubbles is proportional to β. If flow, f, occurs through an area, a, then:

(6) $$f = av$$

If E is constant, then a will be proportional to A. Therefore, with rearrangement of equation 6 and substituting for v from equation 5, we get:

(7) $$f \propto A\beta E$$

When E is constant,

(8) $$f \propto A\beta$$

From equation 5 it is obvious that if E is known, then v can be expressed in cm · s^{-1}. Similarly, if the microvascular CSA is known, then A can be expressed in cm^2. The product of A and v will then represent f in mL · s^{-1}.

Strategies to Test the Model

Ex vivo experiments with explanted veins were initially performed to determine the efficacy of microbubble destruction in a flowing system and to evaluate the optimal PI required to detect flow differences from VI measurements. Because of the large CSA and low resistance of the ex vivo veins, the flow rates used were much higher than those in the microcirculation. To evaluate flow rates seen within the myocardium, in vitro experiments were performed with hollow-fiber bundles that had CSA more akin to that of microvessels. This system was also used to derive the PI versus VI relation at multiple flow rates. To test the model in vivo, we first used an experimental setup in which MBF could be altered without changing CBV. Subsequently, a preparation was used in which changes in MBF were caused solely by changes in CBV. Finally, a coronary stenosis model that more closely resembles the clinical situation was used.

Contrast Echocardiography

Image Acquisition

A prototype Sonos 2500 system (Hewlett Packard) was used for these experiments. All imaging was performed in harmonic mode, in which ultrasound was transmitted at 2 MHz and received at 4 MHz. Ultrasound pulses were gated to an internal timer for the ex vivo and in vitro experiments or to the ECG signal for in vivo experiments. Dual triggering, which allows ultrasound to be transmitted twice within an RR interval, also was used for in vivo experiments to generate short PI. The rationale was to destroy bubbles during the first ultrasound pulse and to image their reappearance within the myocardium with the second pulse. During an imaging sequence, the interval between these pulses was progressively prolonged to allow more bubble replenishment of the ultrasound beam elevation.

The ultrasound transducer was fixed in position with a custom-designed clamp. The transmit power was set at 75% of maximum. The peak negative acoustic pressure at the focal point was 1.1 MPa, and the mechanical index was 0.7. The image depth and transmit focus were each set at 8 cm, and a maximal compression of 60 dB was used. No time-gain or lateral-gain compensation was used. Data were recorded on 1.25-cm videotape with a S-VHS recorder (Panasonic AG-MD830; Matsushita).

Contrast Agent

A second-generation microbubble solution (MRX-115; ImaRx Pharmaceutical) was used in this study and was administered as a continuous infusion in all experiments. The microbubbles have a mean size of 2.5 μm and a concentration of 1.2×10^9 · mL^{-1}. They have an 8-nm bilayer phospholipid shell and are filled with a mixture of air and perfluoropropane. These microbubbles have been shown to have no effect on systemic hemodynamics or pulmonary gas exchange.[5]

Hemodynamic Measurements

All catheters were connected to fluid-filled pressure transducers, which, like the flowmeter, were connected to a multichannel recorder (model ES2000; Gould Electronics). Epicardial coronary artery flows and all pressure signals were acquired digitally at 200 Hz into an 80386-based personal computer via an eight-channel analog-to-digital convertor (Metrabyte). The signals were displayed on-line using Labtech Notebook (Laboratory Technologies).[2]

Flow Measurements

Conduit Flow

Flows in the tubing for the ex vivo and in vitro experiments, as well as to the LAD in the group 1 dogs, were controlled with peristaltic pumps (model 2501–001; Harvard Apparatus, and/or model S10K 2, Sarns Inc). They were measured using time-of-flight ultrasonic flow probes placed directly on the tubing (Series SC, Transonics) or the LAD (Series SB, Transonics).

Nutrient Flow

In group 2 and 3 dogs, the radiolabeled microsphere technique was used as the gold standard for measuring MBF. It was determined by left atrial injection of $\approx 2\times10^6$ 11-μm radiolabeled microspheres (Dupont Medical Products) suspended in a solution of 4 mL of 0.9% saline and 0.01% Tween-80.[1,2] Duplicate reference samples were withdrawn from the femoral arteries over 130 seconds with a constant-rate withdrawal pump (model 944; Harvard Apparatus).

At the end of the experiment, the short-axis slice of the LV corresponding to the echocardiographic image was cut into 16 wedge-shaped pieces, excluding the papillary muscles. Each piece was further divided into epicardial, mid-myocardial, and endocardial segments. The tissue and reference blood samples were counted in a well counter with a multichannel analyzer (model 1282; LKB Wallac), using corrections for activity spilling between energy windows.

MBF to each epicardial, mid-myocardial, and endocardial segment was calculated from the equation $Q_m = (C_m \cdot Q_r)/C_r$, where Q_m is MBF (mL · min^{-1}), C_m is tissue counts, Q_r is rate of arterial sample withdrawal (mL · min^{-1}), and C_r is arterial reference sample counts.[13] Transmural MBF (mL · min^{-1} · g^{-1}) to each of the 16 wedge-shaped pieces was calculated as the quotient of the summed flows to the individual segments within that piece and their combined weight. The perfusion bed of either the LAD or LCx was determined using intracoronary injections of Albunex (Molecular Biosystems).[1,2] Mean MBF to each perfusion bed was then calculated by averaging the transmural MBF in the central 50% to 75% of the pieces in each bed.

Experimental Preparations and Protocols

Ex Vivo Experiments

The aims of these experiments were to demonstrate (1) the efficacy of microbubble destruction by ultrasound in a flow system and (2) the influence of the PI on the detection of flow differences from VI measurements. Fig 3A illustrates our experimental setup. Two segments of external jugular vein (0.8 cm in diameter) obtained from dogs were attached to two separate pieces of 100-cm-long tubing and immersed side-by-side within a water bath. The distance between the veins and transducer was held constant throughout the experiment. The same solution of MRX-115 was circulated continuously through both veins using separate pumps.

In the first experiment, the beaker contained 0.5 mL of MRX-115 in 3 L of 0.9% saline, and the flow rate was held constant in both veins at 52 mL · min^{-1} (flow velocity = 1.7 cm · s^{-1}). Samples of the solutions were withdrawn from the tubing just proximal and distal to the transducer location and immediately placed on a hemacytometer; the number of microbubbles were counted using light microscopy (magnification ×40). In the control stage, no ultrasound was transmitted, whereas in the test stages, it was transmitted using various PI.

In the second experiment, the beaker contained 0.01 mL of MRX-115 in 560 mL of 0.9% saline, which resulted in adequate opacification in the veins without system saturation or attenuation.

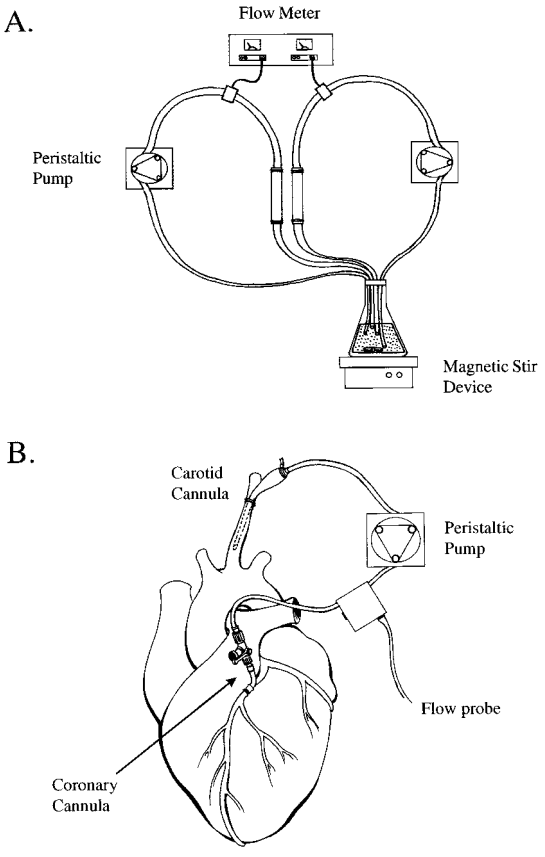

Figure 3. A, Ex vivo experimental setup. B, Animal preparation used for the group 1 dogs.

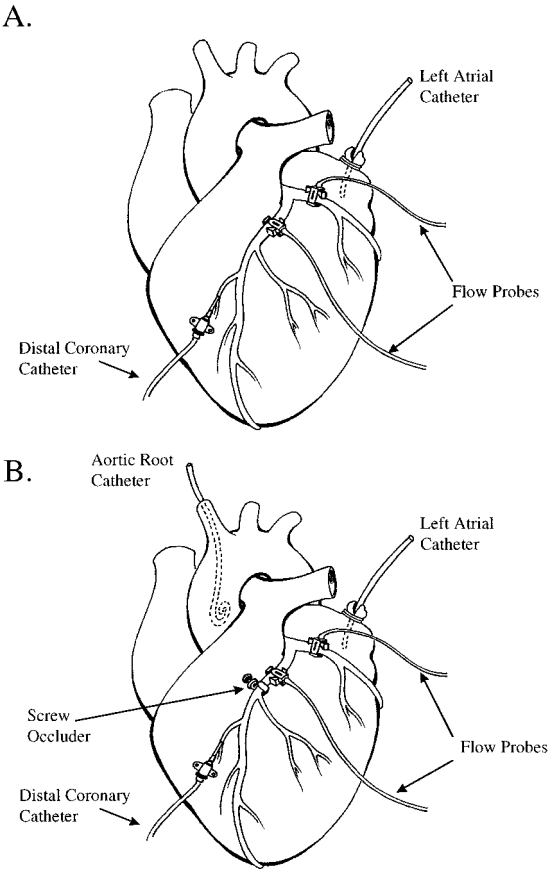

Figure 4. Animal preparations used for the (A) group 2 dogs and (B) group 3 dogs.

The flow in one vein was held constant at 52 mL · min^{-1}, whereas that in the other vein was increased from 52 to 200 mL · min^{-1} in random order, which corresponds to flow velocities ranging from 1.7 to 6.7 cm · s^{-1}. Imaging was performed at PI of 33 and 200 ms.

In Vitro Experiments

The purpose of these experiments was to determine (1) the VI-versus-PI relation for different flow rates and (2) the effect of different microbubble concentrations on the determination of A and β at the same flow rate. The experiments were performed using hollow hemodialysis fiber bundles (Spectra/Por; Spectrum Microgon). A single bundle consists of 352 fibers, each 200 μm in diameter, which is similar to the diameter of the larger myocardial microvessels. Four bundles were attached to tubing and immersed in parallel in a 0.9% saline bath at a fixed distance from the ultrasound transducer.

A solution of 0.2 mL of MRX-115 in 1 L of 0.9% saline was continuously circulated through the bundles using a peristaltic flow pump, and flow rates were varied from 10 to 50 mL · min^{-1}. The PI was varied from 200 to 3000 ms. In one experiment, the concentration of microbubbles was varied while the flow was held constant at 30 mL · min^{-1}. The concentrations of microbubbles in all these experiments did not result in system saturation or attenuation at any PI.

In Vivo Experiments

The study protocols were approved by the Animal Research Committee at the University of Virginia and conformed to the American Heart Association Guidelines for Use of Animals in Research. A total of 21 dogs were used for the experiments. They were anesthetized with 30 mg · kg^{-1} sodium pentobarbital (Abbott Laboratories), intubated, and ventilated with a respirator pump (model 607; Harvard Apparatus). Fluid was administered via 7F catheters placed in the femoral veins. A left lateral thoracotomy was performed, and the heart was suspended in a pericardial cradle.

In group 1 dogs (n=7), the purpose was to define the relation between coronary flow and mean microbubble velocity in a setting in which CBV remains relatively constant. A model with an incised coronary artery (Fig 3B) was therefore chosen because autoregulation is virtually abolished in this model.[1] Accordingly, the proximal LAD was dissected free from the surrounding tissues. A cannula was inserted into the left carotid artery and connected to tubing that was attached to another cannula. After ligation of the LAD, this cannula was inserted into it and secured in place. Flow through the tubing was controlled using a peristaltic flow pump (model 2501–001; Harvard Apparatus) and measured using an extracorporeal time-of-flight ultrasonic flow probe (series SC; Transonics) connected to a digital flowmeter (model T206; Transonics). The LAD flow was adjusted to four to five levels in a random order.

In group 2 dogs (n=5), the purpose was to define the relation between MCE and radiolabeled microsphere–derived MBF in which MBF is altered solely through changes induced in CBV. Accordingly, proximal segments of both the LAD and LCx were dissected free from surrounding tissue. Time-of-flight flow probes (series SB; Transonics) were placed around both vessels, and a 20-gauge catheter (Critikon) was introduced into the LAD via a side branch (Fig 4A). To change MBF, vasodilators were administered directly into the LAD through this catheter using a constant-rate infusion pump (model 944; Harvard Apparatus). Adenosine (Sigma Chemical) was infused at rates of 2.5 μg · kg^{-1} · min^{-1} (low dose) and 5.0 μg · kg^{-1} · min^{-1} (high dose), and acetylcholine (Sigma Chemical Co.) was infused at a rate of 0.3 μg · kg^{-1} · min^{-1}. During the administration of each drug, MCE was initiated only after the LAD flow had stabilized. It was allowed to return to baseline for ≥5 minutes before the next dose/drug was administered. Arterial pressure was monitored via a catheter in the femoral artery.

In group 3 dogs (n=9), the purpose was to determine whether MCE-derived MBF can be used to quantify coronary stenosis severity

TABLE 1. Number of Microbubbles Proximal and Distal to Transducer in Ex Vivo Experiments

	PI, ms			
	Control	33	200	1000	*P*
Proximal to transducer	37±7	37±5	32±3	33±2	NS
Distal to transducer	37±3	0	1±1	17±4	<.001

Number of microbubbles was determined with a hemacytometer.

both at rest and in the presence of coronary hyperemia. Accordingly, these dogs underwent coronary artery dissection similar to that in the group 2 dogs, except that a branch of either the LAD or LCx was cannulated for measurement of distal coronary pressure (Fig 4B). A screw occluder was placed around the vessel to create coronary stenoses of various severities.[2] The severity of a stenosis was judged by the gradient between the central aortic and distal coronary pressure. Three stages were used: baseline and two different degrees of stenoses, which were not flow limiting at rest. At each stage, MCE was performed both before and during an intravenous infusion of WRC-0470, a novel adenosine A_{2a} receptor agonist that causes coronary hyperemia without significant systemic hemodynamic effects.[14]

For MCE, the infusate consisted of 2 mL of MRX-115 in 25 mL of 0.9% saline administered via the femoral vein. This infusion rate resulted in excellent myocardial opacification without saturation or attenuation in any dogs. As soon as a steady state from the infusion of microbubbles was achieved, the imaging protocol, which consists of a sequence of different PI, was initiated. The "imaging" trigger was set to the T wave of the ECG signal (end systole representing the smallest cavity size in the cardiac cycle), whereas the "bubble destruction" trigger was set to different intervals before the imaging trigger. Although both triggers resulted in the production of images that potentially could show myocardial opacification, VI measurements were made only from images captured in end systole.[15] In three dogs, data were also collected with the imaging trigger set to end diastole (peak of the R wave). Regions of interest for the LAD and LCx beds were placed at the same image depth (≈9 to 11 o'clock position for the LAD and 1 to 3 o'clock position for the LCx).

To confirm that the infusions were indeed constant, background-subtracted LV and myocardial VI measurements were performed in three group 1 dogs over 5 minutes and in one group 2 dog over 12 minutes using a PI that has been shown to cause negligible bubble destruction (>1000 ms).[9] The concentration of microbubbles used for the LV VI determinations were lower than that used for the myocardium to ensure that the microbubble concentration versus VI relation was in the linear range.

The relation between VI and microbubble concentration in both the LV cavity and myocardium was evaluated in one dog. The microbubble concentration was slowly increased by changing the infusion rate of a dilute solution of MRX-115 (4 mL in 96 mL of 0.9% saline) from 0.08 to 6.7 mL · min^{-1} in small increments. Imaging was performed with gating to every eighth cardiac cycle (PI of 4.2±0.3 seconds).

Statistical Methods

Comparisons between more than two stages were performed with repeated measures ANOVA, whereas those between two stages were made with Student's *t* test. All correlations were performed using least-squares linear regression analysis. Differences were considered significant at $P<.05$.

Results

Ex Vivo Experiments

Table 1 depicts the efficacy of ultrasound in destroying microbubbles in a flowing system. The number of microbubbles from just proximal and distal to the transducer location were similar when no ultrasound was transmitted. At PI of 33 and 200 ms, virtually no bubbles were seen distal to the transducer. When the PI was increased to 1000 ms, bubble destruction was less.

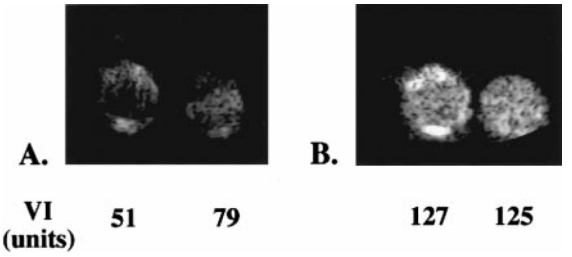

Figure 5. Effect of PI on measured VI in the ex vivo experiment. The vein on the left has one fourth of the flow compared with the vein on the right. The concentration of microbubbles is the same for both veins. More replenishment of microbubbles into the vein with higher flow is seen using a short PI (A), resulting in greater VI disparity between the two veins. When sufficient time is allowed for microbubbles to replenish the beam elevation even in the vein with low flow (B), the VI disparity between the veins is no longer seen. See text for details.

Fig 5 illustrates the importance of using the correct PI for the detection of flow differences based on VI measurements. Although the concentration of microbubbles in both veins was identical, there was a fourfold difference in the flow between the two veins. Fig 5A and 5B depict images acquired at PI of 33 and 200 ms, respectively. At the short PI, more bubbles have replenished the ultrasound beam elevation in the vein with higher compared with lower flow (Fig 5A), allowing for flow differences in the two veins to be noted. In comparison, when the PI was prolonged, the bubbles completely replenished the ultrasound beam elevation in both veins, and flow differences in the two veins were no longer seen (Fig 5B). Obviously, the optimal PI for distinguishing different flows depends on the flow rates themselves.

In Vitro Experiments

Fig 6 illustrates the PI versus VI relations at different flow rates in the hollow fiber bundles. It is obvious that for any flow, several PIs were required to derive the values of β and A. VI increased more rapidly and reached a plateau at a shorter PI when flows were higher (Fig 6A). An excellent linear relation was noted between the value β from the fitted functions and flow measured in the tubing (Fig 6B).

Fig 7 depicts VI data using solutions with three different microbubble concentrations at a constant flow rate of 30 mL · min^{-1}. Two important points are evident from these data. First, as long as the relation between microbubble concentration and VI remains within the linear range,[13] β reflects velocity and is not affected by the concentration of microbubbles infused intravenously. Second, because changing microbubble concentration within the fibers is equivalent to changing the number of fibers containing the same concentration of microbubbles, these results indicate that the measurement of A actually reflects fiber CSA.

In Vivo Experiments

Using a PI >1000 ms, both myocardial and LV video intensities remained unchanged during constant infusions of microbubbles over 5 to 12 minutes. The relations between VI

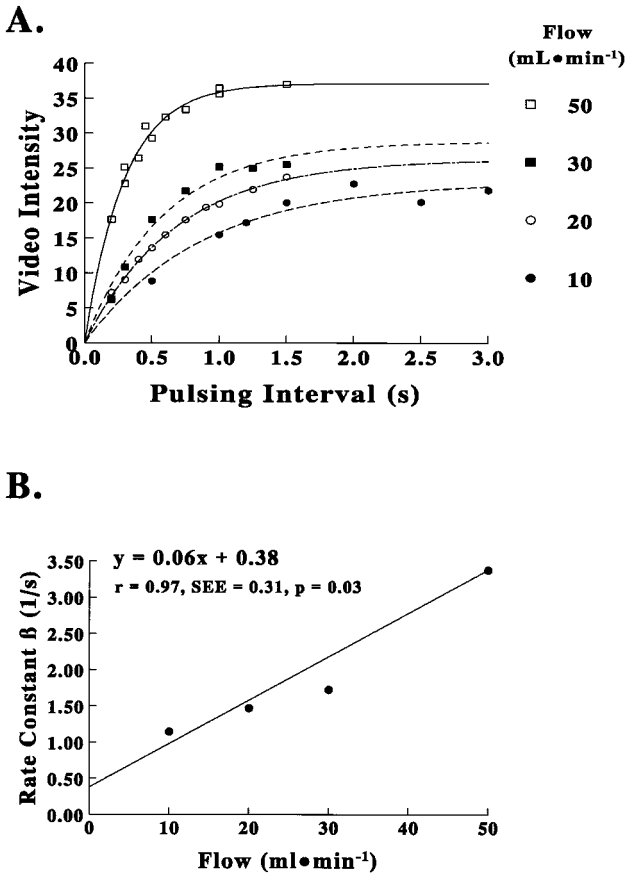

Figure 6. A, PI (*x* axis) versus VI (*y* axis) relation at four different flow rates in the in vitro experiments. B, Relation between absolute flow (*x* axis) and the rate constant β from each of the fitted functions in A (*y* axis). See text for details.

and infusion rate (which denotes microbubble concentration) for both the LV cavity and myocardium are shown in Fig 8. There was an initial rapid rise of VI in the LV cavity as microbubble concentration increased. As the concentration continued to increase, however, the LV VI reached a plateau. Appreciable myocardial opacification was noted only during this plateau phase when microbubble concentration in the LV cavity was high. When the linear portion of the relation between microbubble concentration and VI from the LV cavity was extrapolated to the level at which myocardial VI was

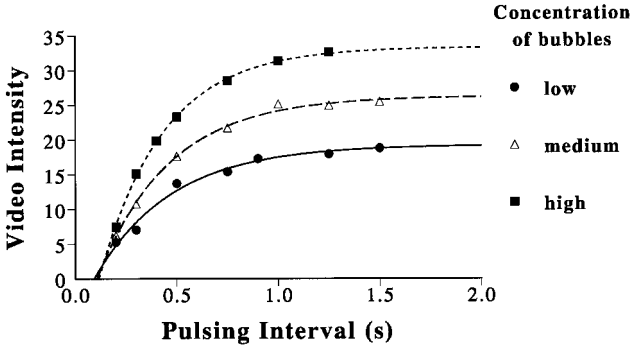

Figure 7. Effect of microbubble concentration on the rate constant β and the plateau VI at a constant flow rate of 30 mL · min^{-1}. The plateau VI increases with the increasing concentration of microbubbles, but the rate constant β does not.

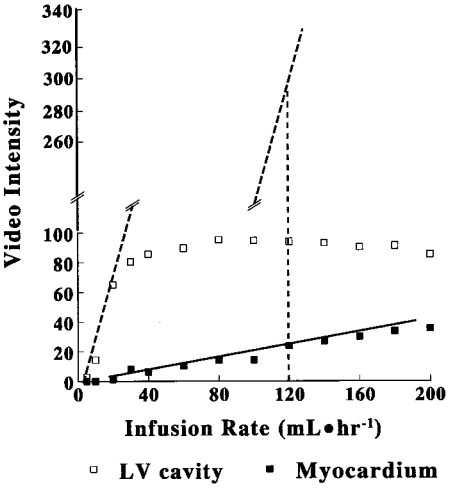

Figure 8. Microbubble concentration (*x* axis) versus VI (*y* axis) relation for both the LV cavity (□) and myocardium (■). Extrapolation of the initial linear portion of the LV cavity relation (dashed line) allows the "expected LV cavity VI" at any microbubble concentration to be estimated. The MBV fraction may be calculated as the ratio between the myocardial VI and the extrapolated LV cavity VI (dotted line). See text for details.

similar to that noted in this study, the myocardial/LV cavity VI ratio was 8%. Because the LV cavity contains only blood, these data indicate that the estimated MBV is 8%. Thus, despite the nonlinear relation between microbubble concentration and VI, myocardial VI can be calibrated as a percentage of the VI in the LV cavity.

Fig 9 depicts images obtained at a constant LAD flow of 65 mL · min^{-1} at four incremental PIs in one group 1 dog. The color-coding algorithm used to illustrate the data has been described previously.[15] Shades of red, progressing to hues of orange, yellow, and then white, represent incremental myocardial contrast opacification. At the shortest PI, no contrast was seen in either the LAD or LCx beds, indicating that the PI was too short to allow replenishment of detectable amounts of microbubbles in either bed. At a higher PI, the VI in the LAD bed increased progressively and reached a plateau at longer PI. Initial opacification of the LCx bed was seen at a higher PI than the LAD bed, and its rate of rise is also slower, indicating a lower microbubble velocity in the LCx bed.

Fig 10A illustrates the VI versus PI plots from the LAD bed at five different flows in one dog. As the LAD flow was increased, the value of β also increased. Fig 10B shows the excellent relation between β and LAD flow in the same dog. Similar results were found in all other dogs (Fig 11) with an average correlation between β and mean coronary flow in all seven dogs of r=.91 (range, .77 to .97).

These results pertain to imaging in end systole only. In the three dogs in which imaging was also performed in end diastole, no differences were found between the value of β derived at end systole or end diastole. Because the interval between the "bubble destruction" and "imaging" pulses can span several cardiac cycles, the rate of replenishment of the ultrasound beam elevation by microbubbles reflects an average of that from different phases of the cardiac cycle, which can explain these findings.

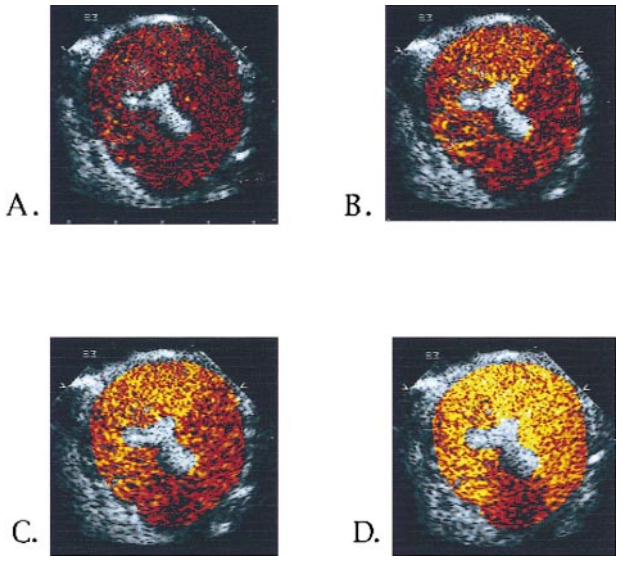

Figure 9. End-systolic images at a constant LAD flow of 65 mL · min^{-1} at four PIs (316, 536, 1608, and 5360 ms in A through D, respectively). At the shortest PI, no contrast can be seen in either LAD or LCx beds, indicating that the PI was too short to allow replenishment of measurable numbers of microbubbles into either bed. VI in the LAD bed progressively increases with increasing PI and plateaus at an interval of 5360 ms. To obtain these color-coded images, three averaged precontrast frames were digitally subtracted from three averaged postcontrast frames at each PI. The VI scale of the resulting subtracted image was expanded to a dynamic range of 128 gray levels, in which the pixel showing the greatest contrast change was assigned a value of 128, and all others were assigned proportionally lower values. All pixels with a gray scale value of >10 were assigned a color based on the degree of contrast enhancement. Shades of red to yellow to orange to white denote greater video intensities. See text for details.

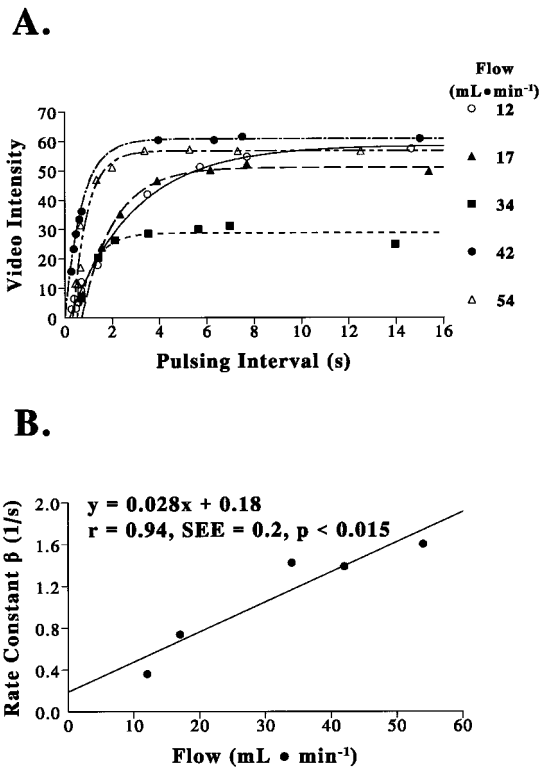

Figure 10. A, Relation between PI (*x* axis) and VI (*y* axis) at five different flow rates from a group 1 dog. B, Relation between the epicardial flow (*x* axis) and the rate constant β derived from the fitted functions (*y* axis) in A for the same dog. See text for details.

MBF was increased in group 2 dogs solely by increasing CBV via intracoronary infusion of vasodilators (adenosine and acetylcholine). The doses of the drugs infused were sufficient to increase LAD flow without any changes in LCx flow or mean arterial pressure (Table 2). During peak hyperemia, both LAD flow and radiolabeled microsphere-derived MBF in the LAD bed increased approximately threefold compared with baseline. An excellent correlation was found in all dogs between the value of β and LAD flow as well as radiolabeled microsphere-derived MBF in the LAD bed (r=.88, P<.001). Despite large increases in MBF caused by the vasodilators, no significant change in A was found, indicating that microvascular CSA within the myocardium did not change appreciably (Table 2). As shown in Fig 12A, the relation between radiolabeled microsphere–derived MBF and MCE derived MBF ($A\beta$) was excellent.

The protocol could not be completed in one group 3 dog due to hemodynamic instability, and the distal coronary catheter resulted in a myocardial infarction in another dog, so the data from the remaining seven dogs are presented in Table 3. There were three stages for each dog: baseline and two separate stenosis stages. Before hyperemia, the pressure gradient across the stenosis increased with increasing stenosis severity, but MBF and all other hemodynamic data remained unchanged. Likewise, the mean values of A, β, and $A\beta$ also did not change at any stage compared with the nonstenosed bed. Thus, like MBF, microbubble velocity and myocardial microvascular CSA remain constant at rest in the presence of non–flow-limiting coronary stenosis.

In the presence of exogenously induced hyperemia with WRC-0470, there were no significant changes in mean aortic pressure or heart rate at any stage compared with the corresponding baseline stage. As expected, the pressure gradient across the stenosis increased significantly (P<.001) in the presence of hyperemia compared with baseline, and this increase was higher for more severe stenoses. MBF to the stenosed bed also increased in all stages with hyperemia, but the maximal hyperemic flow attained before placement of a stenosis was significantly greater (P<.01) than that during either stenosis stage. An excellent correlation was found between β and radiolabeled microsphere–derived MBF for all dogs (mean, r=.93; range, .70 to .99). The value of A from the stenosed bed was lower (P=.05) compared with the control bed with increasing levels of stenosis. The correlation between radiolabeled microsphere–derived MBF and MCE-derived MBF ($A\beta$) for all dogs was excellent (average, r=.93; range, .71 to .99). As shown in Fig 12B, an excellent correlation was also found between the $A\beta$ ratio from the stenosed versus normal bed and the radiolabeled microsphere–derived MBF ratio from the two beds. All the points lie practically on the line of identity except for two outliers (○). In these two dogs, the value of A in the control bed was artificially reduced as a result of lateral wall attenuation, resulting in an apparent "increase" in the $A\beta$ ratio compared with the stenosed bed.

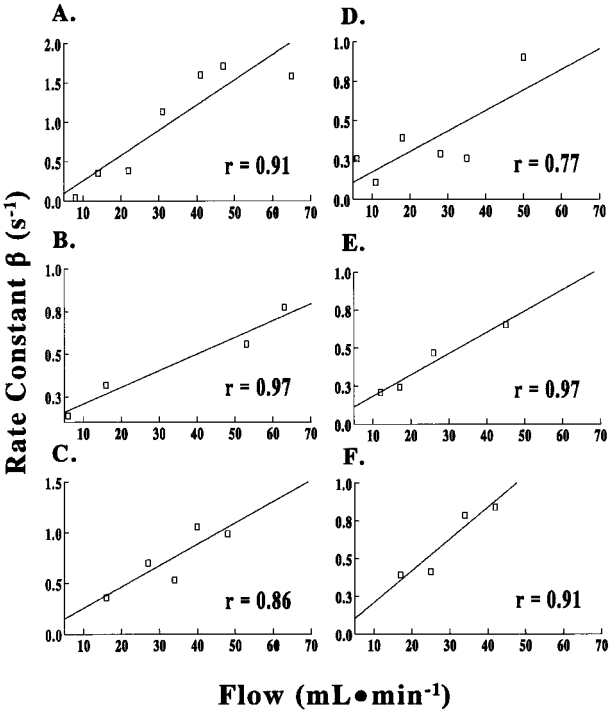

Figure 11. Relation between absolute epicardial flow (*x* axis) and β for the other six group 1 dogs. The average correlation for all seven group 1 dogs was $r=.91$. See text for details.

Discussion

Limitations in Using Tracer Kinetics to Measure Myocardial Perfusion With MCE After Venous Administration of Microbubbles

When microbubbles are injected as a discrete bolus directly into a coronary artery, their mean transit rate reflects the MBF/CBV relation.[1,2] When they are administered intravenously, the input function of the myocardium is the time-intensity curve from the LV cavity. As a result of dispersion of the microbubbles through the myocardial microvasculature, the myocardial output function should be wider than the input function. A number of factors, however, make the myocardial output function appear paradoxically narrower than the input function.

Ultrasound systems have a threshold below which microbubbles are not detected.[13] This threshold results from suppression of electronic "noise," a narrow dynamic range, and compression of the signal to display it on the video monitor. To be detected in the myocardium, therefore, the concentration of microbubbles in the LV cavity must be very high. Because the number of microbubbles in the myocardium is much lower than that in the LV cavity, the threshold effect makes the time-intensity curve from the myocardium appear narrower than that from the LV cavity.[13] This phenomenon makes it impossible to deconvolve the latter from the former, precluding the measurement of the MBF/CBV relation during venous infusion of microbubbles.

Even if the threshold effect were not present, the transit rate of intravenously administered microbubbles would not reflect their dispersion through the myocardium. Microbubbles injected into a peripheral vein first disperse through the cardiac chambers and pulmonary vasculature before reaching the coronary circulation. Compared with the central circulation, further dispersion of the bubbles through the much smaller coronary circulation is therefore insignificant. Consequently, the resulting output function is not much different from the input function,[4] and this difference cannot be resolved by ultrasound. Thus, the measured myocardial output function invariably reflects the dispersion of bubbles in the large central circulation (and hence provides a measure of cardiac output[16]) rather than the mean myocardial transit rate.[4]

Advantages of Our New Approach

The novelty of our approach is that it does not rely on tracer kinetic principles to quantify myocardial perfusion. Destruction of microbubbles and measurement of their reappearance rate within the myocardium during a continuous infusion provide an estimation of mean myocardial microbubble velocity. Similarly, the plateau VI at long PI reflects microvascular CSA. The product of the two provides an estimation of MBF.

The independent estimation of both microbubble velocity and microvascular CSA afforded by our approach also has many advantages, as demonstrated in our study. In situations in which MBF changes are not associated with alterations in CBV, such as in the group 1 dogs, the plateau VI did not change and alterations in MBF were reflected only by changes in microbubble velocity. Similarly, in situations in which MBF changes are associated with changes in CBV but not MBV, the plateau VI should not change. The two examples of this phenomenon in our study occurred during direct coronary infusion of vasodilators in the group 2 dogs and in the presence of non–flow-limiting stenosis at rest in the group 3 dogs. In both instances, reliance on changes in VI alone would have led to errors in the estimation of MBF.

An interesting observation from this study is that when vasodilators were infused directly into a coronary artery, increases in MBF and microbubble velocity were not associated with changes in myocardial microvascular CSA. These real-time in vivo results are identical to those of Crystal et al[18] and Eliasen and Amtorp.[19] In their experiments, the mean myocardial transit rate of red blood cells increased during adenosine infusion, implying that the increase in MBF occurred via increase in CBV, but no changes in MBV were found. The microvessels that are imaged within the myocardium and that constitute MBV are predominantly capillaries,[17] with dimensions or numbers that are not altered by direct coronary infusion of adenosine. Taken together, the results of these studies indicate that direct coronary injection of adenosine increases MBF by dilating microvessels which form a small portion of the MBV or are not present within the myocardia. Thus, by determining both CBV (measurement of the mean transit rate of microbubbles after an intracoronary bolus injection[1,2]) and MBV (measurement of microvascular CSA during an intravenous infusion of microbubbles), MCE could be used to separate changes in capillary dimension or density from those of larger microvessels.

In the presence of coronary stenoses, both microvascular CSA and microbubble velocity were found to be less in the stenosed versus the normal bed during hyperemia. These findings supports those of Canty et al,[20] who measured changes

TABLE 2. Hemodynamic, MBF, and MCE Data in Group 2 Dogs

	Baseline	Mild Hyperemia	Moderate Hyperemia
Heart rate, bpm	124±23	119±24	118±21
Mean aortic pressure, mm Hg*	100±10	97±13	94±7
Mean LAD flow, mL · min^{-1}†	28.0±15.8	59.0±49.2	77.4±56.1
Mean LAD MBF, mL · min^{-1} · g^{-1}†	0.96±0.69	1.75±0.75	2.46±1.15
β†	0.62±0.13	1.32±0.51	1.66±0.86
A*‡	1.0±0.0	1.12±0.14	1.19±0.13
$A\beta$†‡	0.64±0.50	0.97±0.14	2.50±0.74

* No interstage differences noted.
† $P<.01$ between stages.
‡ Normalized to control bed.

in MBV with the use of computed tomography. In the presence of coronary hyperemia, arteriolar dimensions increase with a consequent increase in MBF. In the stenotic bed, however, hyperemia is associated with an increase in the resistance across the bed compared with when no stenosis is present. Thus, a partial collapse of microvessels is likely to occur distal to the arterioles.[6] Our results indicate that one potential site of this phenomenon is the capillary bed.

From the ex vivo experiments, we showed that differences in flow velocity can be detected using a single PI. This approach, however, has two limitations. First, because the magnitude of MBF and the degree of MBF mismatch between beds are not known a priori, the PI used may not be optimal to display the maximal disparity in MBF between the beds. As shown in the ex vivo experiment (Fig 5), use of a PI that is too short or too long may obscure VI disparities. Second, even if optimally timed, a single PI can provide only an assessment of the relative degree of flow mismatch. Multiple PIs are required to quantify myocardial microbubble velocity.

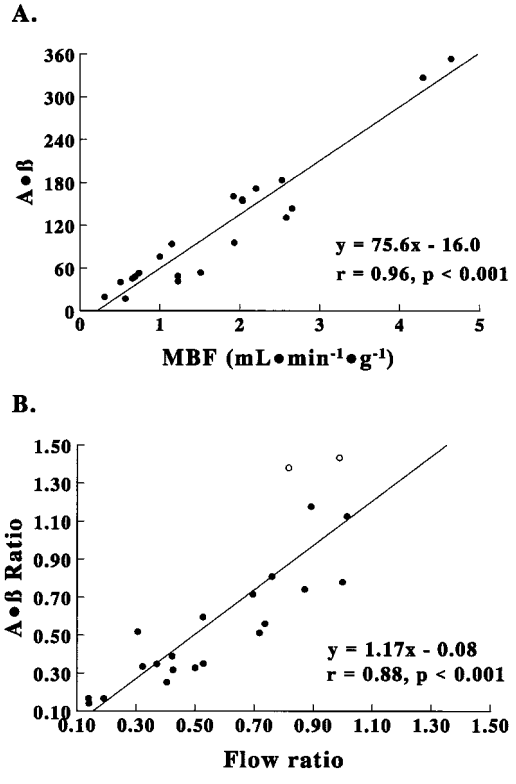

Figure 12. A, Relation between radiolabeled microsphere–derived myocardial blood flow (x axis) and A · β derived on MCE (y axis) in the group 2 dogs. B, Relation between the ratio of radiolabeled microsphere–derived myocardial blood flow from the stenosed and nonstenosed beds (x axis) and the A · β ratio derived on MCE from the two beds (y axis) in the group 3 dogs. See text for details.

Critique of Our Method

We have shown that the myocardial microbubble velocity can be derived from the PI versus VI relation during a continuous venous infusion. Derivation of the absolute value of MBV or microvascular CSA, however, is more involved. First, the VI within the myocardium depends on the concentration of microbubbles infused in the vein. Second, as shown in Fig 8, at concentrations required to produce myocardial opacification, the relation between microbubble concentration and VI within the LV cavity is no longer in the linear range. Thus, unlike other techniques,[21] expression of myocardial VI as a percentage of that obtained from the LV cavity does not provide an accurate estimation of MBV with MCE.

An alternative method for deriving MBV or microvascular CSA is depicted in Fig 8 and is in the range reported with the use of other methods.[2,21] If the sizes of the regions of interest and the ultrasound beam elevation are known, MBF can be calculated in absolute terms. Let us assume that a 1-cm^2 rectangular region of interest is placed over the myocardium and that the ultrasound beam elevation is 0.5 cm; therefore, the volume of tissue being examined is 0.5 cm^3. Using the volume fraction of blood estimated above, MBV will be 0.04 mL. The average myocardial microbubble velocity at rest in our dogs was 0.6 cm · s^{-1}. Tissue flow as derived in equation 7 will therefore be 0.012 mL · s^{-1}, or 0.72 mL · min^{-1}, which is consistent with values derived using radiolabeled microspheres in these dogs.

Because the ultrasound beam profile is not homogeneous along its entire length, it is essential to have the exact value of the beam elevation at all image depths in order to quantify microbubble velocity. This value can be calibrated at different depths using an in vitro system in which both the flow and CSA are known. It may also be possible to "defocus" the beam or alter its profile so the beam thickness becomes more uniform

TABLE 3. Hemodynamic, MBF, and MCE Data in Group 3 Dogs Before and During Induction of Coronary Hyperemia

	No Stenosis	Mild Stenosis	Severe Stenosis	*P*
Before hyperemia				
Mean aortic pressure, mm Hg*	104±12	103±16	92±12	NS
Mean heart rate, bpm*	113±16	109±15	97±12	NS
Mean gradient, mm Hg†	2.0±3.2	10.8±2.6	21.8±14.9	.02
Mean MBF, mL·min^{-1}·g^{-1}†‡	1.0±0.2	1.0±0.2	0.9±0.3	NS
A†‡	1.1±0.2	1.0±0.2	0.9±0.3	NS
β†‡	1.1±0.2	1.0±0.2	0.8±0.3	NS
$A\cdot\beta$†‡	1.2±0.4	1.1±0.4	0.7±0.4	NS
During hyperemia				
Mean aortic pressure, mm Hg*	93±16	91±21	86±13	NS
Mean heart rate, bpm*	121±10	109±15	105±14	NS
Mean gradient, mm Hg†	3.8±3.8	21.2±7.0	33.1±9.7	<.001
Mean MBF, mL·min^{-1}·g^{-1}*‡	0.87±0.13	0.61±0.26	0.34±0.15	<.001
A†‡	1.00±0.22	0.96±0.25	0.71±0.19	.05
β†‡	1.05±0.12	0.58±0.17	0.43±0.17	<.001
$A\cdot\beta$†‡	1.06±0.30	0.54±0.24	0.30±0.13	<.001

* No changes before or during hyperemia at any stage.
† Significant differences before and during hyperemia for at least one stage.
‡ Normalized to nonstenotic bed.

at all depths. In this manner, MBF can be compared from different myocardial beds. We attempted to standardize our comparisons by choosing regions of interest at similar imaging depths.

Cardiac translation, caused by base-to-apex systolic shortening, results in different short-axis planes of the heart being imaged at different times in the cardiac cycle. If imaging is performed using apical views, there also is counterclockwise rotation of the heart during systole. Thus, in either view, the plane in which microbubble destruction occurs may not be precisely the same in which imaging subsequently occurs. This problem can be avoided if both microbubble destruction and imaging are performed at the same point in the cardiac cycle. The entire PI versus VI curve can potentially be constructed using PIs that are multiples of one cardiac cycle. Microbubble destruction and imaging will then occur in the same phase of the cardiac cycle (either end diastole or end systole). Quiet respiration can be used to minimize cardiac motion caused by respiration, and images from the same part of the respiratory cycle can be selected for analysis.

Several PIs are required to derive values for A and β, necessitating several minutes of image acquisition, which makes it essential for systemic hemodynamics and MBF to be stable for a long period. Thus, to produce steady state hyperemia, we selected an intravenous infusion of an adenosine agonist rather than a single venous injection of dipyridamole, because peak hyperemia may not be sustained by the letter. Such an approach may be indicated in the clinical setting as well.

The VI versus PI relations in this study are based on a steady state of microbubble concentration. Unlike a bolus administration of a large dose of microbubbles, in which recirculation of microbubbles is seen,[4–6] prolonged infusions at low concentrations do not change either LV cavity or myocardial VI. It is possible that at these concentrations, the reticuloendothelial system is able to clear the microbubbles from the circulation at a rate that is similar to their intravascular replenishment. Even if a small number of microbubbles escape entrapment, they may not be sufficient to cause an appreciable change in myocardial VI.

Given the <1-mm axial resolution of echocardiography, it may be possible to measure the transmural distribution of MBF. Such an analysis will need the incorporation of both A and β because VI measurements alone were shown not to represent transmural distribution of MBF.[22] The exception to this finding is the situation on which there is damage of the microvessels, so changes in MBF are simply due to changes in microvascular density.[23] Similarly, phasic changes in MBF could also be estimated using this technique if short PI or narrow-beam elevations are used. Abnormalities in phasic changes in MBF may make it possible to detect coronary stenosis at rest without recourse to provocative testing.[24]

Conclusions

We have defined a novel method for measuring microbubble velocity and microvascular CSA that is based on bubble destruction by ultrasound. Measurement of these variables provides a quantitative assessment of MBF using a venous infusion of microbubbles, a technique that is likely to become clinically feasible in the near future. Although these data were derived from the myocardium, this method can be applied to any tissue accessible to ultrasound and therefore has the potential for quantifying perfusion in many organ systems.

Acknowledgments

This work was supported in part by a grant from the National Institutes of Health (R01-HL-48890 and a Grant-in-Aid from the

American Heart Association, Virginia Affiliate. It was also supported by a grant from ImaRx Pharmaceutical Corp (Tucson, Ariz) and an equipment grant from Hewlett Packard Corp (Andover, Mass). The radiolabeled microspheres were provided as a grant from Dupont-Merck (North Billerica, Mass). Dr Wei was the recipient of a Junior Personnel Research Fellowship from the Heart and Stroke Foundation of Canada (Ottawa, Canada), and Dr Firoozan was the recipient of a Junior Research Fellowship from the British Heart Foundation (London, UK). Dr Skyba is supported by postdoctoral fellowship grant F32-HL-095410 from the National Institutes of Health, and Dr Kaul was an Established Investigator of the American Heart Association, National Center. The authors thank Patrick Rafter, MS (Hewlett Packard Corp) for his invaluable assistance and for providing us with the ability to change ultrasound PIs.

References

1. Jayaweera AR, Edwards N, Glasheen WP, Villanueva FS, Abbott RD, Kaul S. In vivo myocardial kinetics of air-filled albumin microbubbles during myocardial contrast echocardiography: comparison with radiolabeled red blood cells. *Circ Res*. 1994;74:1157–1165.
2. Lindner JR, Skyba DS, Goodman NC, Jayaweera AR, Kaul S. Changes in myocardial blood volume with graded coronary stenosis. *Am J Physiol*. 1997;272:H567–H57.
3. Albers VM. *Underwater Acoustic Handbook*. State College, Pa: The Pennsylvania State University Press; 1960.
4. Firschke C, Lindner JR, Wei K, Goodman NC, Skyba DM, Kaul S. Myocardial perfusion imaging in the setting of coronary artery stenosis and acute myocardial infarction using venous injection of a second-generation echocardiographic contrast agent. *Circulation*. 1997;96:959–967.
5. Lindner JR, Firschke C, Wei K, Goodman NC, Skyba DM, Kaul S. Myocardial perfusion characteristics and hemodynamic profile of MRX-115, a venous echocardiographic contrast agent, during acute myocardial infarction. *J Am Soc Echocardiogr*. In press.
6. Wei K, Firoozan S, Jayaweera AR, Linka A, Kaul S. Detection of coronary stenosis from venous administration of microbubbles: Bolus injection or continuous infusion? *Circulation*. 1997;96(suppl I)I-213. Abstract.
7. Kaul S, Senior R, Dittrich H, Raval U, Khattar R, Lahiri A. Detection of coronary artery disease using myocardial contrast echocardiography: comparison with ^{99m}Tc-Sestamibi single-photon emission computed tomography. *Circulation*. 1997;96:785–792.
8. Porter TR, Xie F, Kricsfeld D, Armbruster RW. Improved myocardial contrast with second harmonic transient response imaging in humans using intravenous perfluorocarbon-exposed sonicated dextrose albumin. *J Am Coll Cardiol*. 1996;27:1497–1501.
9. Wei K, Skyba DM, Firschke C, Lindner JR, Jayaweera AR, Kaul S. Interaction between microbubbles and ultrasound: in vitro and in vivo observations. *J Am Coll Cardiol*. 1997;29:1081–1088.
10. Schrope B, Newhouse VL, Uhlendorf V. Simulated capillary blood flow measurement using a non-linear ultrasonic contrast agent. *Ultrason Imaging*. 1992;14:134–158.
11. de Jong N. Higher harmonics of vibrating gas-filled microspheres. In: de Jong N, ed. *Acoustic Properties of Ultrasound Contrast Agents*. The Netherlands: Woerden, Zuidam and Zonen bv; 1993:61–78.
12. Burns PN, Powers JE, Simpson DH, Uhlendorf V, Fritzsche T. Harmonic imaging with ultrasound contrast agents. *Clin Radiol*. 1996;51(suppl):50–55.
13. Skyba DM, Jayaweera AR, Goodman NC, Ismail S, Camarano GP, Kaul S. Quantification of myocardial perfusion with myocardial contrast echocardiography from left atrial injection of contrast: implications for venous injection. *Circulation*. 1994;90:1513–1521.
14. Glover DK, Ruiz M, Yang JY, Koplan BA, Allen TR, Smith WH, Watson DD, Barrett RJ, Beller GA. Pharmacological stress thallium scintigraphy with 2-cyclohexylmethylidene-hydrazinoadenosine (WRC-0470): a novel, short-acting adenosine A_{2A} receptor agonist. *Circulation*. 1996;94:1726–1732.
15. Jayaweera AR, Sklenar J, Kaul S. Quantification of images obtained during myocardial contrast echocardiography. *Echocardiography*. 1994;11:385–396.
16. Galanti G, Jayaweera AR, Villanueva FS, Glasheen WP, Ismail S, Kaul S. Transpulmonary transit of microbubbles during contrast echocardiography: implications for estimating cardiac output and pulmonary blood volume. *J Am Soc Echocardiogr*. 1993;6:272–278.
17. Kassab GS, Lin DH, Fung Y-CB. Morphometry of pig coronary venous system. *Am J Physiol*. 1994;267:H2100–H2113.
18. Crystal GJ, Downey HF, Bashour F. Small vessel and total coronary blood volume during intracoronary adenosine. *Am J Physiol*. 1981;241:H194–H201.
19. Eliasen P, Amtorp O. Effect of intracoronary adenosine upon regional blood flow, microvascular blood volume and hematocrit in canine myocardium. *Int J Microcirc*. 1984;3:3–12.
20. Canty JM, Judd RM, Brody AS, Klocke FJ. First-pass entry of nonionic contrast agent into the myocardial extravascular space: effects on radiographic estimates of transit time and blood volume. *Circulation*. 1991;84:2071–81.
21. Wang T, Wu X, Chung N, Ritman EL. Myocardial blood flow estimated by synchronous, multislice, high-speed computed tomography. *IEEE Trans Med Imag*. 1989;8:70–77.
22. Kaul S, Jayaweera AR, Glasheen WP, Villanueva FS, Gutgessel HP, Spotnitz WD. Myocardial contrast echocardiography and the transmural distribution of flow: a critical appraisal during myocardial ischemia not associated with infarction. *J Am Coll Cardiol*. 1992;20:1005–1016.
23. Villanueva FS, Glasheen WP, Sklenar J, Kaul S. Assessment of risk area during coronary occlusion and infarct size after reperfusion with myocardial contrast echocardiography using left and right atrial injections of contrast. *Circulation*. 1993;88:596–604.
24. Kern MJ, Aguirra F, Bach RG, Donohue TJ, Caraccilo E. Restoration of normal phasic flow velocity after multiple coronary artery stent placement. *Am Heart J*. 1994;127:204–207.